

## Local interaction simulation approach for the response of the vascular system to metabolic changes of cell behavior

M. Scalerandi,<sup>1</sup> G. P. Pescarmona,<sup>2</sup> P. P. Delsanto,<sup>1</sup> and B. Capogrosso Sansone<sup>1</sup>

<sup>1</sup>*INFN-Dipartimento di Fisica, Politecnico di Torino, Corso Duca degli Abruzzi 24, 10129 Torino, Italy*

<sup>2</sup>*Dipartimento di Biologia, Genetica e Chimica Medica, Università di Torino, Via Santena 5 bis, Torino, Italy*

(Received 3 May 2000; revised manuscript received 28 July 2000; published 18 December 2000)

The self-regulatory interactions between cells and the vascular system are mediated by signals propagating at a finite speed. In order to build up a physical model of these processes, several features, such as storing of internal energy, nonclassical nonlinear behavior, and delay and threshold effects, have to be taken into account. Considering cells as particles in different metabolic states according to their internal energy, we have developed a model based on the local interaction simulation approach. Several numerical results, in qualitative agreement with biological observations, illustrate the applicability of the model and the method to implement it.

DOI: 10.1103/PhysRevE.63.011901

PACS number(s): 87.17.-d, 05.45.-a, 02.70.-c

### I. INTRODUCTION

In any biological system, the balance between nutrient supply (depending on the vascularization), nutrient uptake (performed through the receptors), and nutrient consumption (defined by the work performed by stimulated cells) is critical [1]. Upon stimulation, the metabolic state of the cells is modified, e.g., with a variation in consumption, leading to a change in nutrients uptake and blood flow. Nutrients (e.g., glucose and iron) uptake is regulated by their intracellular concentration via a feedback regulation of the receptors numbers [2]. The regulation of the blood flow may be of two types: a short term vasodilating effect mediated by nitric oxide (NO) [3] and a long term angiogenesis (i.e., formation of a neovascular system) mediated by angiogenetic factors [vascular endothelial growth factor (VEGF), angiopoietin, etc.], leading to new vessel formation [4,5]. Both effects introduce a large amount of nonlinearity.

Whenever the feedback between the modulation in the blood flow and receptor number is efficient, the system evolves through quasiequilibrium states. This situation, called self-regulation [6], corresponds to a healthy condition. Pathological causes affect the feedback inducing a transition to a nonequilibrium state and consequent disease. Therefore, understanding the vascular system reorganization induced by metabolic states variations may help in describing, and eventually correcting, the spatiotemporal evolution of pathologies. As an example, it is well-known that local blood flow and, in particular, angiogenesis are crucial for the dynamics of neoplastic growth [7].

In order to describe quantitatively the response of the vascular system to the metabolic changes of the cells behavior, it may be expedient to formulate the above mentioned biological features as physical properties of a dynamical system. However, a detailed description of all microscopic processes is not affordable, but interactions must be defined at a larger (although not macroscopic) scale. An approach of this kind allows us to understand the role of each individual mechanism and their interactions. A basic physical model of our biological system must include a dynamic description of the

cellular properties, their interactions with the environment [8], and the dependence on the local state of the system [9,10].

In particular, cells must be considered as particles which absorb energy from the surroundings (in the form of bound energy in the absorbed molecules) and release it in different ways (by disgregation of chemical bonds) [11]. Due to energy conservation, internal energy may be stored and used later on to build proteins for duplication and/or for damage recovery. The nonlinear interactions with the environment proceed at two different levels, as mentioned before. At an “external” level, cells modulate the elasticity of capillaries and consequently the fluidodynamics of the blood supply. At an “internal” (or cellular) level, the affinity of the cell membrane for a nutrient is adjusted through exploitation of receptors.

External signals (expressed in the form of molecules) induce variations in the particle state. To preserve the energy balance, a feedback is activated by means of internal (“cell generated”) signals. Due to the finite diffusion time of molecules through the different compartments, the system is characterized by a delay in the response. As in many physical systems with a delay, hysteresis appears [12–14]. The effect is nonclassical (i.e., nonanalytically describable) nonlinearity, resembling the behavior recently observed in nonlinear mesoscopic elastic materials subject to an ultrasonic probe [15].

Since an analytical approach is usually inadequate to include all of the above mentioned mechanisms, we propose here a model suitable for numerical simulations. The model is based on the local interaction simulation approach (LISA), which has been successfully applied to the analysis of various physical and biophysical problems, such as wave propagation [16,17], growth phenomena in materials [18,19], and neoplasias [20,21]. In the next section we describe the model and, from the cells and capillaries dynamics, we obtain a set of iteration equations, which allow us to simulate the spatio-temporal evolution of the system, once the initial conditions are assigned. In Sec. III we consider the cases of both short and long term external stimuli (both Gaussian and sinusoidal) and analyze the interplay among the different mecha-

nisms involved. As a result we obtain both classical nonlinear and hysteretic behaviors. The analogy with nonlinear mesoscopic elastic materials may be of some interest, since it also suggests to look in biological systems for the novel effects, which have been discovered in the latter [22].

## II. THE MODEL

We present in this section a physical model for the description of the metabolic states of cells in vascularized tissues. To this purpose, we consider a strip of tissue of length  $L$  and discretize it as a one-dimensional (1D) lattice with  $N = L/\varepsilon$  segments of length  $\varepsilon$ . Each segment is represented by a point (node)  $i (i=1, \dots, N)$  located in its center and is occupied by a number of cells which may belong to different populations. We call  $h_i^t$  the number of (healthy) cells in the segment  $i$  at the time  $t$ . Likewise  $S_i^t$  represents the lateral surface of capillaries in the segment  $i$  at the time  $t$ . Since cells absorb nutrients directly from capillaries, we do not consider the distribution of larger vessels in the specimen. Different values of  $S_i^t$  simulate tissues with different irrigation. Nutrients are assumed to flow inside the capillaries in the strip with a flux  $\Phi^t$ , large enough to remain practically uniform, even when nutrients are consumed in each segment of the strip.

Following the local interaction simulation approach (LISA) [16,20], we specify in the next sections the ‘‘rules of the game,’’ which determine the spatiotemporal evolution of both cells and capillaries. Since we consider only two basic cellular activities (absorption of nutrients from capillaries and their consumption), we may assume that all cell populations behave similarly, i.e., that their evolution is described by the same set of nonlinear iteration equations, albeit with different parameters. In the following we consider only one kind of population ( $h_i^t$ ). The approach, however, may be easily extended to any number of populations, including cases, such as tumoral cells, for which some biological processes are inhibited (i.e., the corresponding parameters vanish).

### A. Cell dynamics

As already mentioned in the Introduction, cells behave as particles with an internal energy depot. For the specific problem considered in this paper, it is convenient to classify cells as belonging to four possible states: normal (characterized by a minimum energy consumption), active (when an external stimulus requires additional work), mitotic (when the internal stored energy is used for duplication), and apoptotic (corresponding to cell death). The amount of transformed energy defines the transition from a normal to an active state (in general active states have a continuum energy distribution), while a threshold process involving the internal energy determines a transition into a mitotic or apoptotic phase.

Nutrient absorption is performed by cell receptors. In the process molecules are brought from the outside into the internal part of the cell, increasing the cell energy in the form of bond energy of the absorbed molecules. The number  $\Gamma_i^t$  of receptors formed by each cell is defined by the required

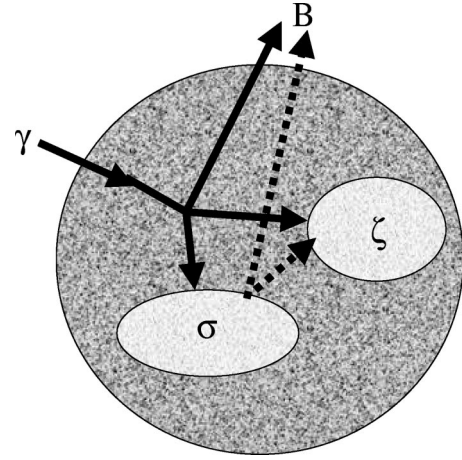


FIG. 1. Schematic representation of the mechanisms involved in the transformation from an extracellular to an intracellular nutrient.

amount of nutrients: cells consuming more nutrients develop a larger number of receptors [6]. Each receptor absorbs a given amount of nutrient  $\delta$  during each time step  $\tau$ . In general, the number of receptors on the cell surface is larger than the minimum required for performing the task assigned to the cell. However, not every receptor is active, since their activation depends on the concentration of nutrients in the neighborhood of the cell. The energy absorbed in the segment  $i$  in the time step ( $t \rightarrow t + \tau$ ) is

$$\Delta_i^t = \gamma_i^t h_i^t, \quad (1)$$

where

$$\gamma_i^t = \Gamma_i^t \delta \left[ 1 - \exp\left(-\frac{\Phi^t S_i^t}{h_i^t \Gamma_i^t \delta}\right) \right]. \quad (2)$$

The exponential term is included in order to keep into account the partial inactivation of receptors.

The nutrient incorporated by the cell corresponds to an internal energy [23], which is rapidly processed within the cell nucleus, via three different channels (see Fig. 1):

(i) a certain amount of nutrient molecules is broken and the corresponding energy  $B_i^t$  is released, allowing the cell to perform a given metabolic function induced by an external or internal stimulus requiring an energy  $\Omega_i^t$ . Normally  $B_i^t = \Omega_i^t$ , unless cells are damaged, as discussed later;

(ii) a second part, corresponding to an energy  $\zeta_i^t$ , is stored in the cell (e.g., as glycogen production in muscles, fats accumulation, etc.);

(iii) the remainder energy  $\sigma_i^t$  is used for protein synthesis in order to recover from damage or, if it becomes sufficiently large, to activate the cell cycle and induce mitosis (cellular duplication). The three processes are hierarchically defined, i.e., the second and third occur only if nutrients are left over after the previous one(s).

Even in the resting state cells have a very high metabolic rate, which is required not only for performing specific functions, but also for keeping structure and shape [24]. In normal conditions,  $\gamma_i^t$  is slightly larger than  $B_i^t$ , since, other-

wise, the cell could not cope with small environmental variations. In fact, small reductions in the absorption can quickly result in a lethal event for the cell. As a consequence, energy storing is normally active. Biological considerations suggest that the process be described by means of an oscillatory function [23]:

$$\zeta_i^t = \tilde{\zeta}_i^t \left[ 1 + \cos\left(\frac{2\pi}{T}t\right) \right]. \quad (3)$$

In many situations the external stimulus acts on a time scale  $\tilde{T}$  which is orders of magnitude larger than the oscillation period  $T$ . Since the time unit  $\tau$  is chosen for computational reasons as a small (but not too small) fraction of  $\tilde{T}$ , it is still much larger than  $T$ . Then,  $\zeta_i^t$  may be replaced by its average value  $\tilde{\zeta}_i^t$ , which has an upper limit  $\tilde{\zeta}_0$ . The oscillations amplitude is restricted by the intracellular nutrient availability. Since the stored energy  $\sigma_i^t$  may be exploited whenever the nutrient  $\gamma_i^t$  falls below the required amount  $\Omega_i^t + \tilde{\zeta}_0$ , the available nutrient  $\nu_i^t$  at each time  $t$  is

$$\nu_i^t = \gamma_i^t + \sigma_i^t. \quad (4)$$

It follows

$$\tilde{\zeta}_i^t = \begin{cases} \tilde{\zeta}_0 & \text{if } (\nu_i^t \geq \Omega_i^t + \tilde{\zeta}_0) \\ \nu_i^t - \Omega_i^t & \text{if } (\Omega_i^t < \nu_i^t < \Omega_i^t + \tilde{\zeta}_0) \\ 0 & \text{if } (\nu_i^t \leq \Omega_i^t). \end{cases} \quad (5)$$

Next, we define a total consumption per cell

$$\beta_i^t = B_i^t + \zeta_i^t. \quad (6)$$

It follows

$$\sigma_i^{t+1} = \sigma_i^t + \gamma_i^t - \beta_i^t, \quad (7)$$

with  $\beta_i^t$  driven by an extracellular or intracellular stimulus.

The stored energy is, however, utilized mainly as an immediate remedy when the nutrient is not sufficient. For a longer term solution, when the nutrient is too low or the consumption too large, the cell exploits another mechanism, i.e., the expression of more receptors in order to adapt to the changing environment. The process is reversible, when nutrient absorption again compensates consumption. Therefore the number of receptors oscillates between a minimum  $\Gamma_-$  and a maximum  $\Gamma_+$ . The process is well-described by the following iteration equation:

$$\Gamma_i^{t+1} = \Gamma_i^t + k_\Gamma \mu_i^t \sum_{s=\pm} (1 - e^{-(\Gamma_i^t - \Gamma_s)}) \Theta(s \mu_i^t), \quad (8)$$

where

$$\mu_i^t = \Omega_i^t + \zeta_i^t - \gamma_i^t. \quad (9)$$

$\Theta(x)$  is the Heaviside function and  $\mu_i^t$  represents the difference between required and available nutrient, which may be in turns positive or negative. The parameter  $k_\Gamma$  affects the

delay in the variation of the number of receptors with respect to variations in the consumption (delay of the signaling system).

Despite the increasing number of receptors, large variations in the consumption (e.g., due to large efforts) can lead to the condition  $\zeta_i^t = \sigma_i^t = 0$  and  $\mu_i^t > 0$ . As a consequence, some cells can no longer perform their function and cellular damage may occur. Damaged cells satisfy their requirement (signal) only partially, i.e., they participate in the metabolism at a reduced rate. To mimic this process, we assume that, in the case of damage:

$$B_i^t = \gamma_i^t < \Omega_i^t. \quad (10)$$

A long term and strong damage induces accumulation of toxic compounds which may produce cellular death (apoptosis) [6]. Here we limit ourselves to consider the kind of abrupt apoptosis, which may occur when the stimulus suddenly requires a disproportionated amount of energy. Under this condition  $B_i^t$  may fall below a survival threshold  $B_0$ . It follows

$$h_i^{t+1} = h_i^t \exp\left[-k_B \frac{B_0 - B_i^t}{B_0} \Theta(B_0 - B_i^t)\right]. \quad (11)$$

During the decreasing metabolism phase, the receptors reabsorption is delayed. Consequently absorption becomes larger than consumption and  $\sigma_i^t$  may increase. In a rather short time, damaged cells recover and, eventually, upon reaching a given threshold  $\sigma_0$ , cellular duplication (mitosis) occurs:

$$h_i^{t+1} = h_i^t \exp\left[k_\sigma \frac{\sigma_i^t - \sigma_0}{\sigma_0} \Theta(\sigma_i^t - \sigma_0)\right]. \quad (12)$$

The latter, however, is a very slow process and usually takes place only to compensate a previous apoptotic stage. Otherwise it seldom happens in healthy tissues, since it is usually inhibited by the strong activity of the cells and consequent nutrient storage and consumption, before the amount necessary for duplication is reached.

The state diagram of the cell is represented in Fig. 2 in the  $\gamma - \Omega$  plane. The points in the plot represent different cell conditions and the arrows show the corresponding metabolic oscillation amplitudes. Note that their lengths vary according to their distance from the diagonal  $\gamma = \Omega$ . The region of apoptosis is below the line  $\gamma = B_0$ .

In the discussion above, we have implicitly assumed the same behavior for all cells belonging to the same segment. Cells, however, are not homogeneous; in fact they display a different behavior according to their age: older cells have a lower metabolism and capability of expressing new receptors. In our treatment these individual differences are not explicitly considered, but averaged out statistically. For example, damage is distributed at the same rate among all cells belonging to a given segment.

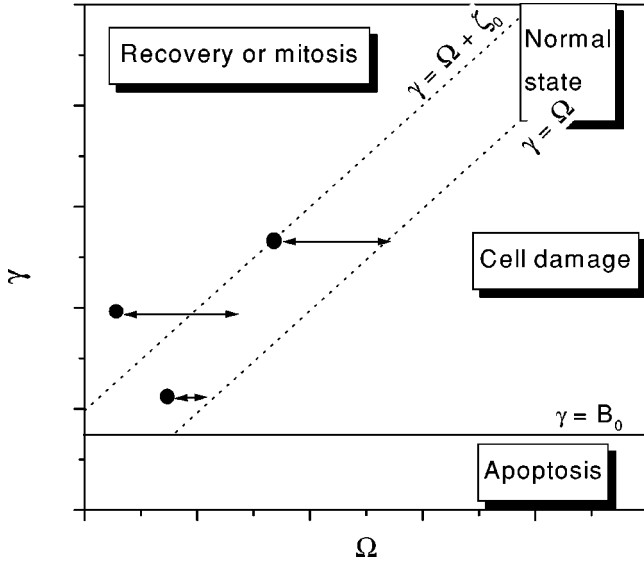


FIG. 2. Cell state diagram in the stimulus-absorption plane  $(\Omega, \gamma)$ . Dotted lines represent the phase transition boundaries between different behaviors. Self-regulating systems usually lie in the region between dotted lines.  $\sigma$  is assumed to be zero (not enough nutrient to leave a remainder).

### B. Capillaries dynamics

The aim of the vascular system is to supply the different organs with an amount of blood sufficient to cope with their actual needs (oxygen and/or nutrients). Variations in the local nutrient consumption cause a redistribution of the capillaries lateral surface along the tissue. In fact as a response to the deficiency of blood supply, cells, while increasing their affinity for nutrients (e.g., activating more receptors), also produce specific molecules, such as nitric oxide and vascular endothelial growth factor (VEGF), which induce local vasodilatation.

Unless the formation of new vessels is considered, the global amount of capillaries in the tissue must be constant. Therefore a local vasodilatation corresponds to vasoconstriction somewhere else in the tissue. In order to simulate this process, we assume that capillaries “diffuse” and redistribute the excess of nutrients:

$$F_i^t = \Phi^t S_i^t - \Delta_i^t, \quad (13)$$

in order to keep it uniform in the tissue

$$S_i^{t+1} = S_i^t + \sum_{\pm} \frac{\alpha_i^{\pm}}{\Phi^t} (F_{i\pm 1}^t - F_i^t), \quad (14)$$

where  $\alpha_i^{\pm}$  are the local diffusion coefficients to the right and left directions, respectively.

Finally, the equations for the time evolution of the flux must be defined. Generally  $\Phi$  is kept constant by the supplying system (e.g., liver, lungs, etc.). However, since the metabolic system has an upper threshold  $\Psi$ , when consumption increases the consumed nutrient may no longer be completely restored, leading to flux reduction (i.e., hypoxia or starvation):

$$\Phi^{t+1} = \Phi^t + k_{\Phi} \left( \Psi - \sum_i \Delta_i^t \right) \Theta \left( \sum_i \Delta_i^t - \Psi \right). \quad (15)$$

### C. Initial conditions

The initial conditions are assumed to correspond to a system in a stable and resting condition, with a constant number of cells and without any pathology or activated specific functions. The number of cells is constant, due to a balance between the (small) number of dying and duplicating cells: in fact the resting state may be defined by that condition. Initially a given amount of cells  $h_i^0$  is defined in each node for each cells population. The initial consumption is assumed to be just sufficient to perform the vital cell functions and the number of receptors is assumed to provide  $\gamma_i^0 = B_i^0 + \zeta_i^0$ . The available nutrient per node  $\Phi^0 S_i^0$  is initially larger than the absorption  $\Delta_i^0$ . The initial distribution of the capillaries sections is defined as

$$S_i^0 = \frac{F_i^0 + \Delta_i^0}{\Phi^0}, \quad (16)$$

where  $F_i^0$  is the initial excess of nutrient, assumed to be uniform along the tissue.

## III. RESULTS AND DISCUSSION

We present in this section a few examples of applications of the model and analyze the spatiotemporal evolution in the distribution of capillaries and in the number of receptors exploited by the cells when an external stimulus is applied to the system, assumed to be self-regulating. To mimic different environmental conditions (metabolic states), we have varied the initial excess nutrient  $F^0$ , keeping fixed the other parameters, which are listed here with their values in arbitrary (but consistent) units:

$$\alpha_i^{\pm} = 0.2, \quad \phi^0 = 1, \quad \Psi = 6000,$$

$$\Gamma_i^0 = 0.055, \quad \tilde{\zeta}_0 = 0.005, \quad \delta = 1, \quad h_i^0 = 10,$$

$$\sigma_0 = 1, \quad \tau = 1, \quad \Gamma_+ = 0.35, \quad \Gamma_- = B_0 = 0.05,$$

$$k_{\Gamma} = 0.5, \quad k_{\sigma} = \ln 2, \quad k_B = 1, \quad k_{\Phi} = 1.$$

We discretize the tissue as a 1D strip with  $N=1000$  segments and consider both a single shot and a periodic external stimulus:

$$\Omega_i^t = 0.05 + 0.1 \cdot e^{-[(t-500)^2/10^6]} \cdot e^{-[(t-2000)^2/10^6]} \quad (17)$$

and

$$\Omega_i^t = 0.05 \left[ 1 + e^{-[(t-500)^2/10^6]} \cdot \sin\left(\frac{2\pi}{1000}t\right) \right], \quad (18)$$

respectively.

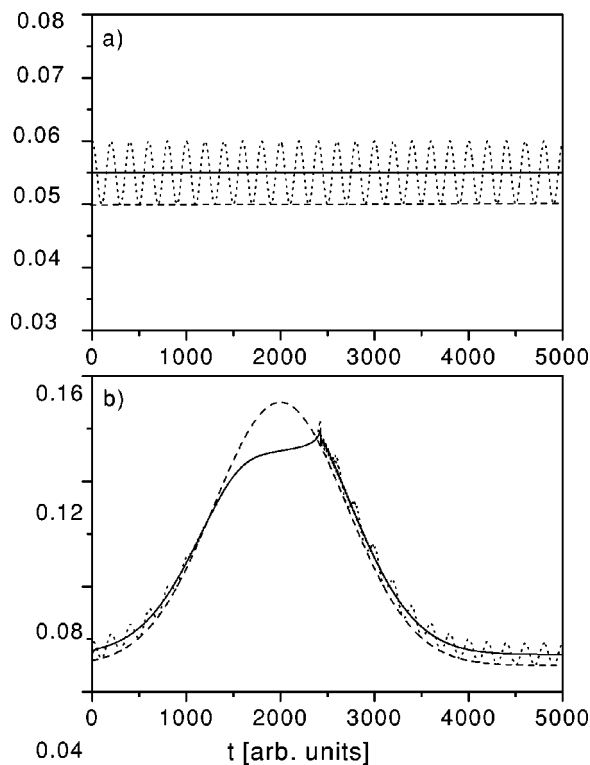


FIG. 3. Time evolution of  $\gamma$  (solid line),  $\Omega$  (dashed line), and  $\beta$  (dotted line) for a given segment  $i$ . (a): system without external stimulus. (b): system with a Gaussian external stimulus.

#### A. Effects of a short term external stimulus

In this section we consider changes in the cell metabolic state acting on a time scale comparable with the internal oscillation period. Short and repeated stimuli are the most likely events in living organisms. For the sake of notational simplicity, we omit, in the following, the indices  $i$  and  $t$ .

In Fig. 3 we analyze the effect of an external Gaussian stimulus applied for a time interval  $\Delta t = 5000\tau$ , corresponding to 25 cell oscillations of period  $T = 200\tau$ . Figure 3(a), shown only for reference, illustrates the case of a system of cells in rest. In the absence of an external stimulus, the nutrient absorption  $\gamma$  (solid line) is constant and the consumption  $\beta$  (dotted line) is oscillating according to Eq. (3). Since the consumption is always larger than the metabolic requirement ( $\Omega = B = B_0$ ), fat or glycogen accumulation (proportional to the area between the oscillations and the dashed line) takes place.

When the external stimulus is applied  $\gamma$  increases since the number of receptors increases: see Fig. 3(b). However, due to saturation in the number of receptors,  $\gamma$  trails behind the applied stimulus (dashed line) and the oscillations  $\zeta$  die away. At about  $t = 1300\tau$ , cell damage begins. When the stimulus levels off, at about  $t = 2500\tau$ , receptors are slowly reabsorbed and the oscillations  $\zeta$  start again. Notice the peak in  $\gamma$ , due to recovery effects. Phenomena such as vasodilation, apoptosis, etc. are almost negligible in this case and will be studied in the next section.

It is remarkable that cell self-regulation does not occur when cells are overfed or resting. In both cases, in fact, fat or

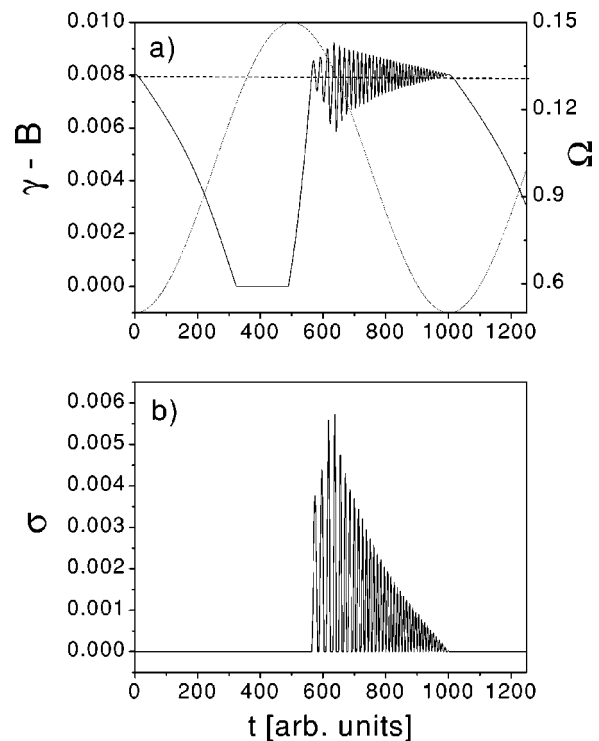


FIG. 4. Time evolution of  $\gamma - B$  (solid line, upper plot, left scale) and  $\sigma$  (lower plot) for a sinusoidal signal  $\Omega$  (dotted line, upper plot, right scale). In the upper plot  $\zeta_0 = 0.008$  is reported for reference (dashed line).

glycogen accumulates as expected. By contrast, excessive stimuli or hypoxia induce starvation and cellular apoptosis. Consequently, biological systems always lie in a critical region, where their functionality balances their interaction with the environment.

The situation in which a sinusoidal stimulus is applied is different, since periodical oscillations in the cell metabolism induce permanent modifications in the environment and in the number of receptors exploited. As a consequence of the various regulation mechanisms, nonperiodical oscillations in the intracellular and stored nutrient appear. To illustrate this effect, the behavior of a system subject to 1 1/4 cycles of a sinusoidal stimulus is analyzed in Fig. 4. The difference between absorption and consumption  $\gamma - B$  is reported in Fig. 4(a) (solid line). Three phases may be easily identified. In the first one ( $0 < t < 300$ )  $\gamma$  is larger than  $B$ , all cells adapt to the stimulus; oscillations (filtered out in the plot through averaging) are capable of coping with the excess intracellular nutrient. As a consequence, the amount of stored nutrient  $\sigma$  remains zero [as shown in Fig. 4(b)]. In the second phase ( $300 < t < 500$ )  $\gamma = B > B_0$  and  $B < \Omega$ , the system starts suffering for the excess stimulus. As a consequence some cell damage occurs, while most of the remaining cells are sufficiently well fed. During the releasing phase ( $500 < t < 1000$ ), the increased nutrient availability causes  $\gamma > B$  up to when  $\gamma - B > \zeta_0$ , i.e., metabolic oscillations are no longer sufficient to consume all the incoming intracellular nutrient. As a consequence storage of nutrient ( $\sigma$ ) occurs. However,  $\sigma$  is progressively used up (as noticeable in the successive

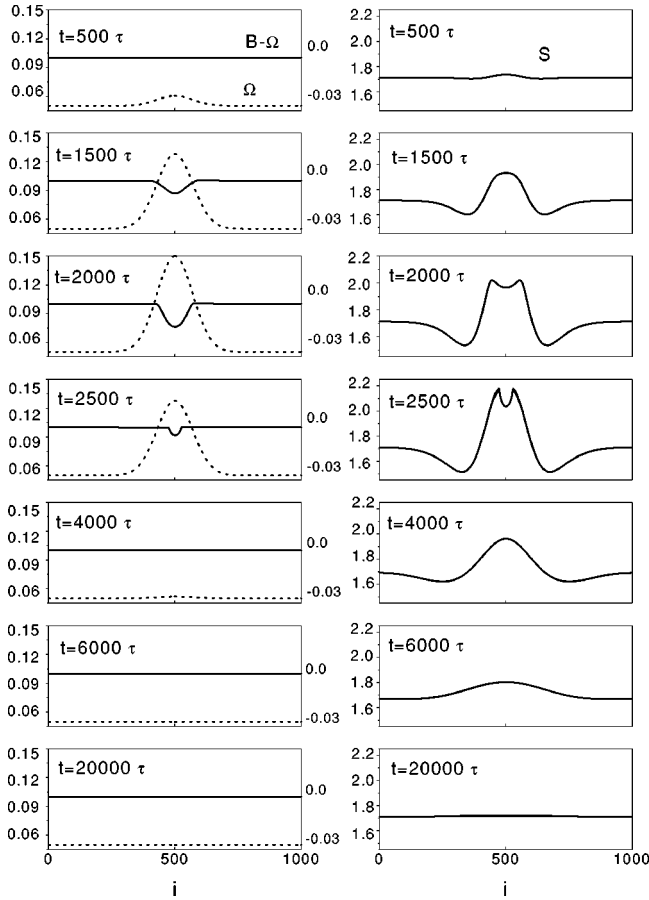


FIG. 5. Time evolution of a system excited by an external Gaussian stimulus (several snapshots). Left column: cell damage, proportional to  $B - \Omega$  (solid line, right scale) and  $\Omega$  (dashed line, left scale); right column: redistribution of the capillaries lateral surface  $S$ .

depletions), since the cell consumes it instead of expressing receptors and for damage recovery. Consequently  $\gamma - B$  oscillates with varying amplitude.

In the case of Fig. 4, the nutrient (accumulated for DNA synthesis) never reaches the threshold for mitosis. However, in other cases in which apoptosis had previously occurred, mitosis can be observed, corresponding to a rejuvenation of the system. This is consistent with the fact that an organ which is not used ages and loses its capability to perform its biological functions.

**B. Effects of a long term external stimulus**

When the external stimulus acts over a time scale much larger than the period  $T$  of the cell oscillations, the latter becomes negligible, as already remarked. However, effects such as vasodilatation and receptors expression become important.

In Fig. 5 we consider the cell damage due to an external Gaussian stimulus, assumed to be proportional to  $\Omega - B$  (solid line, left column), and to the spatial distribution of capillaries lateral surface (right column). Initially, the metabolic level  $B$  is up to the stimulus  $\Omega$  (dashed line) and only a slight vasodilation effect is visible in the region corre-

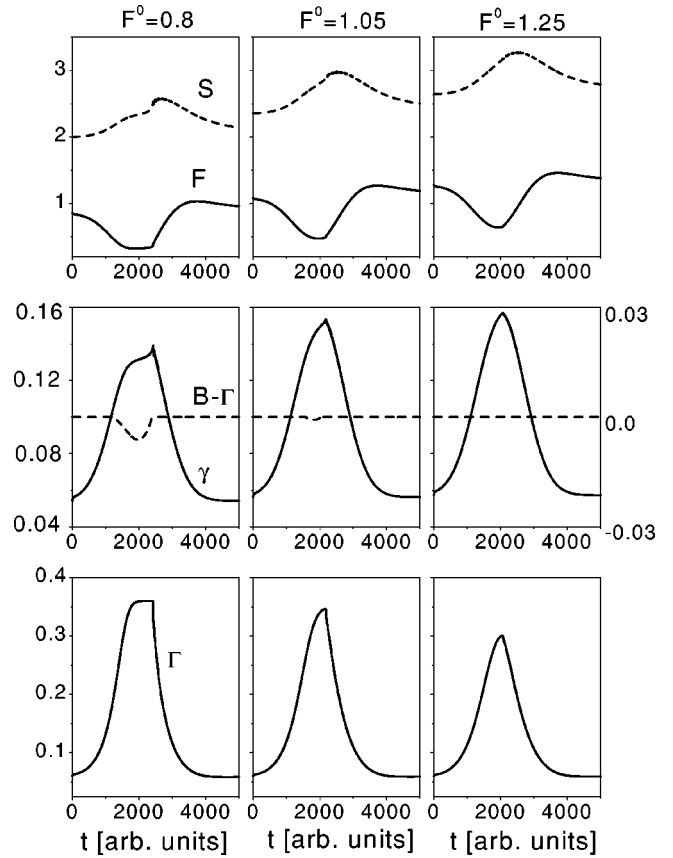


FIG. 6. Time evolution of a system excited by an external shot for three values of the initial excess nutrient  $F^0$ . First row: excess nutrient  $F$  (solid line) and capillaries surface  $S$  (dashed line); second row: absorbed nutrient  $\gamma$  (solid line) and damage  $B - \Omega$  (dashed line); third row: number of receptors  $\Gamma$ .

sponding to larger nutrient consumption (around  $i = 500$ ). As a consequence, the capillary sections decrease in the surrounding region. Successively, the applied stimulus induces strong metabolic changes, which cannot be afforded by older cells. Consequently the latter are partly damaged around the center of the specimen, as shown in the snapshots at  $t = 1500\tau$  and  $2000\tau$ . As a consequence, the vasodilatation stimulus stops in the corresponding region (right column at  $t = 2000\tau$ ). Later ( $t = 2500\tau$ ) a rapid recovery occurs bringing back cells to their normal metabolic state. The sections evolution is strongly delayed with respect to the external stimulus, reaching a maximum of dilatation at  $t = 2500\tau$ , when the metabolic phase is already decreasing. At later times, the stimulus is completely removed and the capillary distribution returns slowly to its initial distribution.

The local evolution of the system can be analyzed by plotting the relevant quantities versus time at a selected location (i.e., for a selected group of cells). In Fig. 6 we consider the time evolution at  $i = 500$  (center of the specimen) due to a Gaussian external stimulus, given by Eq. (17) and represented by a dashed line in Fig. 3(b), for three different environmental conditions:  $F^0 = 0.8, 1.05,$  and  $1.5$  arbitrary units (in the three columns, respectively). The three cases represent systems with increasing preexistent vascularization.

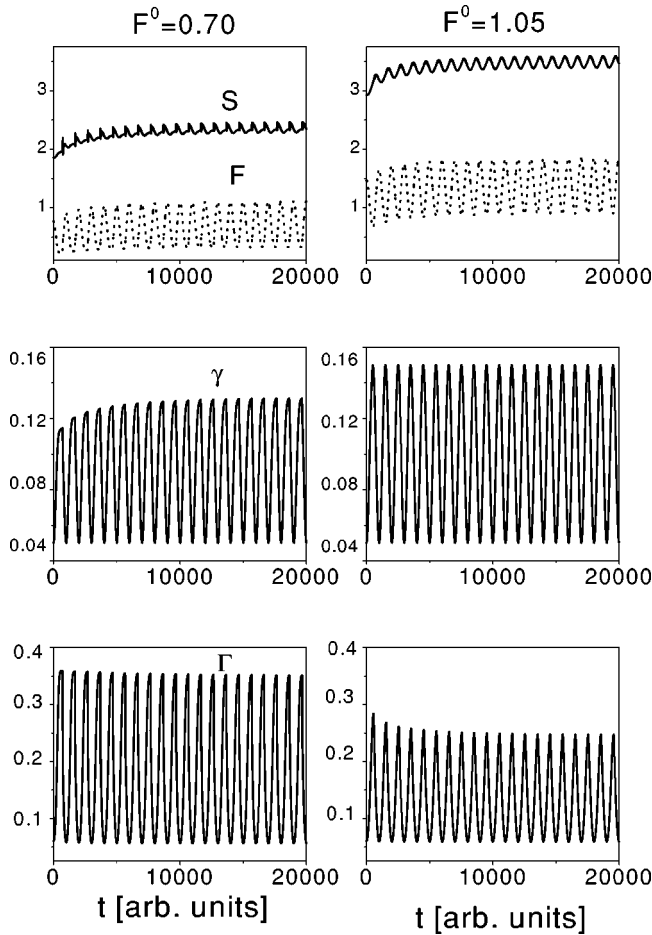


FIG. 7. Time evolution of a system excited by an external sinusoidal stimulus for two values of the initial excess of nutrient  $F^0$ . First row: capillaries surface  $S$  (solid line) and excess of nutrient  $F$  (dotted line); second row: absorbed nutrient  $\gamma$  (solid line); third row: number of receptors  $\Gamma$ .

If the system is well fed (third column), the absorption  $\gamma$  and also, to a lesser degree, the number of receptors  $\Gamma$  follow the stimulus  $\Omega$ . Since  $B = \Omega$ , no cell damage occurs.  $F$  initially follows the behavior of  $\gamma$  (although with opposite sign), but due to the slow increase of the local vascularization  $S$ , the curve is not quite symmetric in its way up. Notice also the large time delay (of about  $500\tau$ ) in the peak (vasodilatation) of  $S$ .

If the system is underfed (first column),  $\gamma$  cannot keep up with  $\Omega$  and a behavior, such as in the bottom plot of Fig. 3, ensues. As a consequence, cell damage occurs, since  $B < \Omega$ . In correspondence with the discontinuous behavior of  $\gamma$ , due to the end of the recovery process ( $B = \Omega$ ), cusps may also be observed in the plots of  $F$  and  $S$ . The number of receptors  $\Gamma$  increases up to when it reaches saturation, as shown by the plateau in the bottom plot, then it starts decreasing with a very small delay, due to reabsorption. The value  $F^0 = 1.05$  (second column) represents the intermediate optimal case between the two cases ( $F^0 = 0.8$  and  $F^0 = 1.25$ ) discussed so far.

In Fig. 7 the effect of a long term sinusoidal stimulus [Eq. (18)] is analyzed. The plots show the time evolution in  $i$

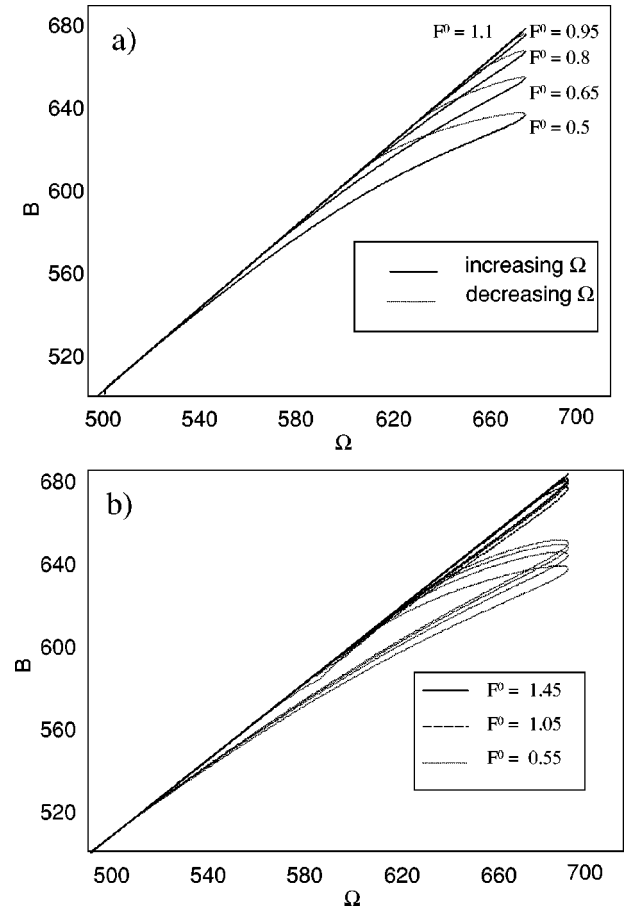


FIG. 8. Total consumption of the system  $B$  vs  $\Omega$ . (a) external Gaussian stimulus; (b) external sinusoidal stimulus.

$= 500$  of  $S$  and  $F$  (first row),  $B$  (second row), and  $\Gamma$  (third row). As expected, all quantities display an oscillatory behavior with the same frequency as the stimulus. In addition we observe that  $S$  is subjected to a ‘‘dynamic hysteresis’’ [14], i.e., oscillates around a mean value, which slightly increases up to an asymptotic value. Such an effect is due to the delay of vasodilatation: in fact at the end of each cycle  $S$  does not return to its initial value (as already noticed in Fig. 4) and so, during the following cycle, the system is advantaged in adapting to the stimulus. As a consequence, a similar behavior is found for  $B$ , while the number of exploited receptors decreases with time due to a larger efficiency in activation.

### C. Hysteretic behavior

The classical nonlinear response of the system under investigation is due to the partial damaging which increases with the applied stimulus. In addition, the system displays a hysteretic behavior assimilable to a memory of the past history, which eventually disappears when the stimulus is removed [25]. The delay of the signaling system is responsible for such a behavior.

In Fig. 8(a) the curves  $B$  versus  $\Omega$  are reported for a Gaussian stimulus  $\Omega$  and five different initial vascularization densities. As expected, for large values of the initial vascu-

larization ( $F^0=1.1$ ), the system behaves linearly: the response of the system to the organism requirements is complete. In the other cases, the delay in receptors formation causes nonlinearity. The difference in the slopes between the increasing and decreasing curves is due to a different recovery versus damage rate [see Eqs. (8) and (12)] at different stimulus levels. We observe that both the hysteretic (area of the loop) and classical nonlinearity increase with decreasing  $F^0$ . We remark here that the hysteretic behavior is not induced by the discontinuity in the receptors formation and reabsorption [Eq. (8)], since similar hysteretic loops have also been obtained in preliminary models without such a discontinuity (results not reported here for brevity).

Conditioning effects in the hysteretic behavior are induced on the system when a periodic stimulus is applied, i.e., when repeated loops are performed consecutively without relaxation between successive cycles. In Fig. 8(b),  $B$  is plotted versus  $\Omega$  for a sinusoidal signal for three values of  $F^0$ . As observed previously, a delay in the response of the vascular system causes a variation of the nutrient distribution at the beginning of each successive cycle. As a consequence, the hysteretic loop moves upward, up to an asymptotic limit loop, closer to the linear behavior than the one corresponding to the first cycle. As in the case of Fig. 8(a), the nonlinearity decreases when  $F^0$  increases. A similar behavior has been observed in quasistatic stress versus strain cycles in nonlinear mesoscopic elastic materials [26].

#### IV. CONCLUSIONS

The purpose of our work was to build up a physical model of self-regulatory mechanisms in the feeding behavior of a group of cells supplied with  $O_2$  and other nutrients by a vascular tree. The self-regulatory behavior allows local adjustments of the nutrient supply to the cells of the tissue; the intensity of stimulation and local availability of specific nutrients drive the cells in the direction of work (e.g., mechanical, secretory) or of proliferation. In our model the link between all these functions is the intracellular concentration of energy. The higher energy limit corresponds to a concentration that allows cells to duplicate (mitosis). We assume that mitosis takes place only when this concentration is reached, whether by increasing the blood flow or receptor number, or by decreasing the intracellular breakdown threshold.

The lower energy limit is the concentration below which cells undergo apoptosis (programmed death), releasing mol-

ecules into the environment as nutrients for the surrounding cells. When the nutrients concentration is confined between these two limits, the cell is alive and can perform work and regulate both the number of receptors and NO synthesis, increasing both of them when the nutrient decreases.

Cellular work induced by an external stimulus requires consumption of intracellular energy that must be replaced. An increased number of receptors and increased blood flow cooperate to accomplish this function, in agreement with the results of our simulations. Likewise, in both real tissues and in our simulations the increased consumption in one area induces a shift of the flow from the surrounding resting areas to the active one. Thus in both areas the flow corresponds to the consumption, the excess nutrient  $F$  is constant and the system automatically reaches a new steady state. When the stimulus is released, the system returns to the resting condition.

Since nutrients uptake or blood flow changes require a certain amount of time due to the finite molecules diffusion speed, an activated system needs time to reach a new steady state. A similar lag phase is required to return to the resting state. The resulting hysteretic behavior has been found (see Fig. 8) to be strongly dependent on the local conditions, namely the excess nutrient  $F^0$ .  $F^0$  depends on the previous history of the tissue and incorporates both the nutrient concentration and capillaries surface. The hysteretic behavior is more pronounced when  $F^0$  is low. This behavior is the rule in physiological systems (e.g., respiration at the pulmonary level). Evolutionary pressure always pushes biological systems to work in conditions of limited nutrients supply or, equivalently, biological systems have evolved to perform the maximal possible work in any given environment compatibly with the available amount of nutrients.

The model proposed is based on the definition of the state diagram of the cell. The temporal evolution of the cell behavior corresponds to a trajectory in the state diagram. Several forms of disease can be described through a variation of the parameters which define the state diagram [27].

#### ACKNOWLEDGMENTS

This work has been partly supported by the INFM Parallel Computing Initiative. The authors also wish to thank Professor C. A. Condat (FAMAF, Argentina) for useful discussions and suggestions.

- 
- [1] P. Ponka and C. N. Lok, *Int. J. Biochem. Cell. Biol.* **31**, 1111 (1999).
  - [2] H. C. Lee and Y. H. Wei, *J. Biomed. Sci. (Basel)* **7**, 2 (2000).
  - [3] L. J. Ignarro, G. Cirino, A. Casini, and C. Napoli, *J. Cardiovasc. Pharmacol.* **34**, 879 (1999).
  - [4] S. C. Ballara, J. M. Miotla, and E. M. Paleolog, *Int. J. Exp. Pathol.* **80**, 235 (1999).
  - [5] R. S. Kerbel, *Carcinogenesis* **21**, 505 (2000).
  - [6] M. A. Aon and S. Cortassa, *Dynamic Biological Organization* (Chapman and Hall, London, 1997), Chap. 9.
  - [7] S. C. Ferreira, M. L. Martins, and M. J. Vilela, *Physica A* **272**, 245 (1999).
  - [8] P. S. Landa and A. Rabinovitch, *Phys. Rev. E* **61**, 1829 (2000).
  - [9] C. Suguna, K. K. Chowdhury, and S. Sinha, *Phys. Rev. E* **60**, 5943 (1999).
  - [10] G. Fath and Z. Domanski, *Phys. Rev. E* **60**, 4604 (1999).
  - [11] F. Schweitzer, W. Ebeling, and B. Tilch, *Phys. Rev. Lett.* **80**, 5044 (1998).
  - [12] V. N. Kukudzhinov, *Mech. Solids* **34**, 58 (1999).



- [13] M. N. Krainik, L. S. Kamzina, and S. A. Flerova, *Phys. Solid State* **42**, 944 (2000).
- [14] B. K. Chakrabarti and M. Acharyya, *Rev. Mod. Phys.* **71**, 847 (1999).
- [15] R. A. Guyer and P. A. Johnson, *Phys. Today* **20**, 30 (1999).
- [16] P. P. Delsanto, R. B. Mignogna, M. Scalerandi, and R. S. Schechter, in *New Perspectives on Problems in Classical and Quantum Physics*, edited by P. P. Delsanto and W. A. Saenz (Gordon and Breach, New Delhi, 1998), Vol. 2, pp. 971–977.
- [17] P. P. Delsanto and M. Scalerandi, *J. Acoust. Soc. Am.* **104**, 2584 (1998).
- [18] M. Scalerandi, P. P. Delsanto, and C. F. Pirri, *Philos. Mag. B* **80**, 507 (2000).
- [19] M. Scalerandi, S. Biancotto, and P. P. Delsanto, *Comput. Phys. Commun.* **97**, 195 (1996).
- [20] M. Scalerandi, A. Romano, G. P. Pescarmona, P. P. Delsanto, and C. A. Condat, *Phys. Rev. E* **59**, 2206 (1999).
- [21] P. P. Delsanto, A. Romano, M. Scalerandi, and G. P. Pescarmona, *Phys. Rev. E* **62**, 2547 (2000).
- [22] G. C. Kember, G. A. Fenton, K. Collier, and J. A. Armour, *Phys. Rev. E* **61**, 1816 (2000).
- [23] M. Katsumata, K. A. Burton, J. Li, and M. J. Dauncey, *FASEB J.* **13**, 1405 (1999).
- [24] I. Prigogine and G. Nicolis, *Q. Rev. Biophys.* **4**, 107 (1971).
- [25] R. A. Guyer *et al.*, *Phys. Rev. Lett.* **74**, 3491 (1995).
- [26] E. Ruffino and M. Scalerandi, *Il Nuovo Cimento B* (in press).
- [27] B. Capogrosso Sansone, P. P. Delsanto, G. P. Pescarmona, and M. Scalerandi (work in progress).